energies

Article

Optimal Dispatch of Agricultural Integrated Energy System with Hybrid Energy Storage

Wu Yang [1], Yi Xia [1], Xijuan Yu [1], Huifeng Zhang [1], Xuming Lin [1], Hongxia Ma [1], Yuze Du [2,*] and Haiying Dong [2]

[1] Linxia Power Branch of State Grid Gansu Electric Power Company, Linxia 731100, China
[2] School of New Energy and Power Engineering, Lanzhou Jiaotong University, Lanzhou 730070, China
* Correspondence: duyuzelanzhou@163.com

Abstract: Rural energy is an important part of China's energy system, and, as China's agricultural modernization continues, integrated agricultural energy systems (AIES) will play an increasingly important role. However, most of China's existing rural energy systems are inefficient, costly to run, and pollute the environment. Therefore, meeting various agricultural energy needs while balancing energy efficiency and costs is an important issue in the design and dispatch of integrated agricultural energy systems. In conjunction with hybrid energy storage (HES), which has been developed and matured in recent years, this paper proposes a new type of AIES structure and optimal dispatching strategy that incorporates HES, biogas generation (*BG*), P2G, and an electric boiler (*EB*) to provide new ideas for problem solving. Firstly, the structure of AIES is introduced and the mathematical model of the equipment of the system is described; then, an economic optimal dispatching model with the objective of minimizing the comprehensive operating costs of the system is established, and the output of each piece of energy conversion equipment is controlled to achieve the effect of improving the system's operating performance and reducing the operating costs. The results show that the system with HES and multi-energy coupling equipment has a 20% lower overall cost, 23.2% lower environmental protection cost, and 51% higher energy efficiency than the original system; the stored power of energy storage equipment in the HES mode is primarily determined by the change in demand of the corresponding load, and the number of conversions between different energy sources is limited. The energy conversion loss is minimal.

Keywords: integrated energy system; agricultural park; hybrid energy storage; optimal dispatch

check for updates

Citation: Yang, W.; Xia, Y.; Yu, X.; Zhang, H.; Lin, X.; Ma, H.; Du, Y.; Dong, H. Optimal Dispatch of Agricultural Integrated Energy System with Hybrid Energy Storage. *Energies* **2022**, *15*, 9131. https://doi.org/10.3390/en15239131

Academic Editors: Nicu Bizon and Abu-Siada Ahmed

Received: 19 October 2022
Accepted: 26 November 2022
Published: 2 December 2022

1. Introduction

According to statistics, over 1.9 billion people live in developing countries in South Asia and Africa, with rural areas accounting for 80% of the population in these regions [1]. The rise of rural populations and economies in developing nations in recent years has rendered the traditional power supply model insufficient for power generation and environmental protection, resulting in a poor energy consumption mix, low consumption levels, and low energy efficiency. Areas supported by agro-industries in Pakistan and India are still heavily reliant on traditional energy sources; in remote areas and small islands in the United States, a relatively small rural population has the highest electricity costs in the country; and in Western China, although some rural areas have been modernized, clean energy use is low [2]. In brief, agricultural power system architecture must be based on local natural resource endowments in order to achieve complementarity between diverse energy sources and boost energy efficiency [3]. Integrated agricultural energy systems (AIES) provide creative solutions to this challenge. In recent years, the demand for agricultural parks to build multi-energy complementary systems with HES has become increasingly strong. Compared with the extension of the traditional power grid, the development of renewable energy systems (RES) with multiple energy complements in agricultural parks has significant economic and environmental benefits [4–7]. Wang et al. [8] took the economic and environmental operation of the system as the goal, added various energy conversion equipment to the distributed agricultural park, and established a mathematical model of the distributed system. The example proved that the model could well solve the problems of poor economic benefits and large emissions of pollutants caused by the extensive operation of the agricultural park. Huang et al. [9] put forward a hierarchical control framework for AIES based on the cooperation of energy storage and cogeneration, proving that the system with energy storage can minimize the cost of power purchases and consume redundant photovoltaic power generation. In terms of system energy storage forms and parameter selection, Mitali J et al. [10] comprehensively summarized the technical principles and operating characteristic parameters of thermal, electrical, and methane energy storage. Kamal M M et al. [11] compared four AIES models based on environmental and economic indicators and carried out a sensitivity analysis on each parameter. Finally, according to the results of the example, they gave the reference value for the optimal allocation of agricultural energy storage. In addition to setting up multiple types of energy storage in the agricultural park system, the application of biomass power generation and multi-energy coupling equipment can also achieve low-cost renewable energy consumption in the agricultural park, which can improve the flexibility of system operation.

Because of its low raw material supply cost and environmental protection characteristics, biogas is widely used for heating and power generation in agricultural systems [12,13]. Ding et al. [14] studied the utilization mode of biogas resources, comprehensively evaluated the energy-saving effect of biogas digesters in the multi-energy coupling system, and proved that the construction of biogas digesters plays an important role in changing the consumption structure of the AIES. Jamil Ahmed et al. [15] modeled the AIES, including wind power, photovoltaic, biogas, and energy storage, and the calculation example verified that the consumption rate of renewable energy in this scenario was close to 100%. Bamisile O et al. [16] proved that the RES, including innovative CPVT, wind energy, and biomass power generation, can not only reduce carbon dioxide emissions, but also improve the overall energy utilization efficiency of the system. The introduction of *P2G* equipment and an electric boiler into the integrated energy system (IES) can improve the operational economy and stability of the system [17,18]. Paper [19] proposed an IES with electric heating, *P2G*, and gas storage equipment, and studied the multi-objective optimization operation method of IES with multi-energy flow coupling. Luo F et al. [20] proposed an IES optimization strategy with *P2G* and other equipment, which solves the problems of the operation scheduling scheme and energy storage configuration priority. The promotion effect of different energy storage configurations is analyzed from the perspective of the operating economy of IES, which reduces the cost of waste wind power and environmental pollution. The literature [21,22] discusses the economic optimization under the gas–electricity HES mode, analyzes the correlation between the energy storage output and various energy load demands, and considers the complementarity between multi-energy conversion equipment and multi-energy storage equipment. The above research proves that the development of RES with multiple energy complementarities has certain economic and environmental benefits. However, most of the IES models proposed for agricultural parks only consider a single BES, rarely use *P2G* and other coupling equipment, and rarely use HES equipment with heat storage and gas storage equipment.

To summarize, this paper constructs a comprehensive AIES model. The system includes *P2G*, *EB*, *BG*, an MG-CHP unit, and HES equipment. In order to solve the coordination and scheduling problems among photovoltaics (*PV*), wind power (WP), cogeneration, *P2G*, and HES, the strategy takes the minimum total operating cost as the objective function and the wind and solar power generation forecast and load demand forecast curve as the input, and optimizes the system economy, protects the environment, and improves energy efficiency by controlling the output of various types of energy conversion equipment. Finally, the correctness and effectiveness of the method are verified by an example.

2. AIES Structure with HES and Its Equipment Model

2.1. The AIES Structure

The external input energy of the AIES includes wind energy, solar energy, electricity, biomass energy, and natural gas. Load types include electric, thermal, and gas loads. The main energy conversion equipment includes the MG-CHP units, electric boilers, *P2G* equipment, etc. The system structure is shown in Figure 1. WP, *PV*, and *BG* units are directly connected to the system, and MG-CHP units provide heat and power for the park; EB and *P2G* equipment provides heat and gas, respectively, through electricity consumption. The energy storage equipment of the system includes BES, HST, and GST.

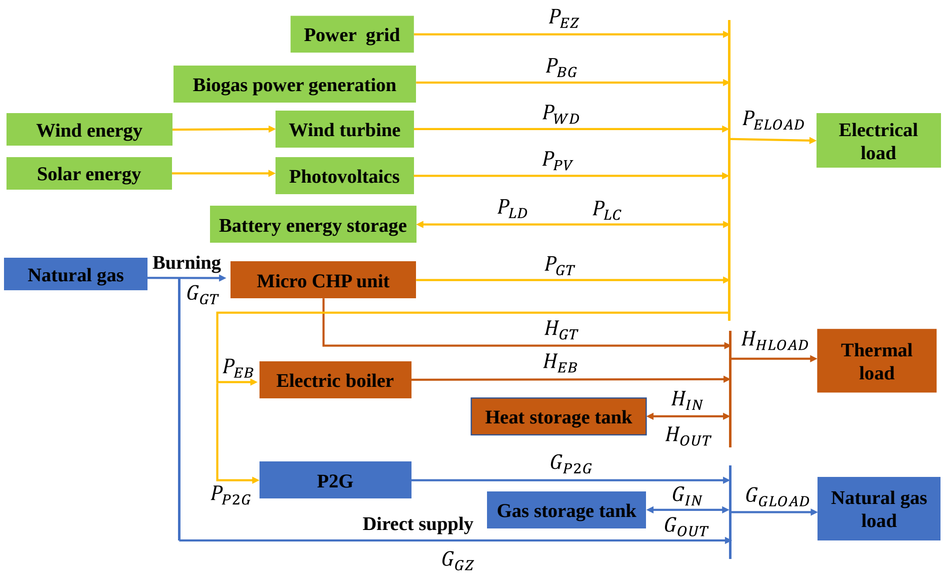

Figure 1. The AIES structure.

2.2. Equipment Model of AIES

1. MG-CHP unit

The MG-CHP unit generates electricity by burning natural gas, and its mathematical model is as follows:

$$G_{GT}(t) = \frac{P_{GT}(t) \cdot \Delta t}{\eta_E^{GT} \cdot R_G} \tag{1}$$

where G_{GT} is the consumption of natural gas, m^3; P_{GT} is the output electric power of the MG-CHP unit during the time period, kw; η_E^{GT} is the generation efficiency of the unit; R_G is the low calorific value constant of natural gas, taken to be 9.7 kWh/m^3 [23].

The relationship between the electric and thermal output of the MG-CHP unit in the t period is as follows:

$$H_{GT}(t) = \frac{1 - \eta_E^{GT} - \eta_{LOSS}^{GT}}{\eta_E^{GT}} \eta_B P_{GT}(t) \Delta t \tag{2}$$

where H_{GT} is the thermal output power of the MG-CHP unit, kw; η_{LOSS}^{GT} is the heat dissipation loss rate of the unit; η_B is the heating coefficient.

2. Electric boiler

$$H_{EB}(t) = P_{EB}(t) \eta_{EB} \Delta t \tag{3}$$

where H_{EB} is the heating power, kw; P_{EB} is the power consumption, kw; η_{EB} is the heating efficiency.

3. *P2G*

$$G_{P2G}(t) = \frac{P_{P2G}(t) \cdot \Delta t \cdot \eta_{P2G}}{R_G} \tag{4}$$

where G_{P2G} is the natural gas output of $P2G$ equipment in t time, m^3; P_{P2G} is the power consumption, kw; η_{P2G} is the gas generation efficiency.

4. Biogas power generation unit

$$\begin{cases} E_{BG}(t+1) = E_{BG}(t) - P_{BG}(t)\Delta t \\ 0 \leq E_{BG} \leq E_{BG,\max} \\ 0 \leq P_{BG}(t) \leq P_{BG,\max} \end{cases} \tag{5}$$

where P_{BG} is the output of the biogas power generation unit, kw; $P_{BG,\max}$ is the upper limit of unit power, kw; E_{BG} is the remaining generation capacity of the biogas generator unit, kw·h; $E_{BG,\max}$ is the maximum capacity, kw·h.

5. Battery energy storage

$$\begin{cases} E_{ESS}(t) = E_{ESS}(t-1) + \left(P_{LC}\eta_C - \frac{P_{LD}}{\eta_D}\right)\Delta t \\ E_{ESS,\min} \leq E_{ESS} \leq E_{ESS,\max} \\ 0 \leq P_{LC} \leq u_{ess}P_{LC,\max} \\ 0 \leq P_{LD} \leq (1-u_{ess})P_{LD,\max} \end{cases} \tag{6}$$

where E_{ESS} is the storage capacity in t period, kw·h; η_C and η_D represent the charging and discharging efficiency, respectively; P_{LC} and P_{LD} represent the charging and discharging power of stored energy, kw, respectively; $P_{LC,\max}$ and $P_{LD,\max}$ represent the maximum charging and discharging power of stored energy, kw; u_{ess} is a binary variable to avoid simultaneous charging and discharging.

6. Heat storage tank

$$\begin{cases} Q_{HS}(t) = Q_{HS}(t-1) \cdot (1-\vartheta_{HS}) + \left(H_{IN}(t) \cdot \eta_{IN} - \frac{H_{OUT}(t)}{\eta_{OUT}}\right) \cdot \Delta t \\ 0.2Q_{HS,\min} \leq Q_{HS} \leq 0.8Q_{HS,\max} \\ 0 \leq H_{IN} \leq u_{HS}H_{IN,\max} \\ 0 \leq H_{OUT} \leq (1-u_{HS})H_{OUT,\max} \end{cases} \tag{7}$$

where Q_{HS} is the residual capacity of the heat storage pool, kw·h; ϑ_{HS} is the self exothermic efficiency; H_{IN} and H_{OUT} are the heat transfer and release power in the time period, kw; η_{IN} and η_{OUT} are the heat transfer and heat release efficiency. u_{HS} represents the heat storage state of the pool.

7. Gas storage tank

$$\begin{cases} V_{GS}(t) = V_{GS}(t-1) + (G_{IN}(t) - G_{OUT}(t))\Delta t \\ 0 \leq G_{IN} \leq u_{GS}G_{IN,\max} \\ 0 \leq G_{OUT} \leq (1-u_{GS})G_{OUT,\max} \\ 0 \leq V_{GS} \leq 0.9V_{GS,\max} \end{cases} \tag{8}$$

where V_{GS} is the remaining gas storage capacity of the tank, m^3·h; G_{IN} is the intake gas volume, m^3; G_{OUT} is the amount of gas released, m^3. u_{GS} represents the gas storage state of the tank.

3. Optimal Dispatching Model of AIES

3.1. Objective Function

On the basis of satisfying the energy demand of users, this paper considers multiple types of energy conversion equipment to participate in the energy supply and realize the complementary supply of multiple energy sources to minimize the system's comprehensive cost F. The objective function F includes the energy purchase cost F_1; environmental pollution cost F_2; and equipment loss cost F_3. The details are as follows:

$$\min F = F_1 + F_2 + F_3 \tag{9}$$

$$\begin{cases} F_1 = \sum_{t=1}^{24} S_{EB}\, P_{EZ} + \sum_{t=1}^{24} S_{EG}\,(G_{GT} + G_{GZ}) \\ F_2 = \sum_{i=1}^{m} v_{ci} d_{ci} \sum_{t=1}^{24} P_{GT}(t) \\ F_3 = \sum_{s,t} P_{s,t} C_{op}^{s} \end{cases} \tag{10}$$

where S_{EB} is the grid electricity sales price; S_{EG} is the unit price of natural gas; P_{EZ} is the direct purchasing power; G_{GZ} is the power of directly purchased natural gas; m is the number of pollutant types; v_{ci} is the unit emission control cost of pollutant i; d_{ci} is the emission of j pollutants generated by the unit output of the MG-CHP unit; $P_{s,t}$ is the output of equipment S at time t; C_{op}^{s} is the unit output loss cost of equipment S.

3.2. Constraints

- Electrical power balance constraint.

$$P_{EZ} + P_{PV} + P_{WD} + P_{BG} + P_{LD} + P_{GT} = P_{ELOAD} + P_{P2G} + P_{LC} + P_{EB} \tag{11}$$

where P_{ELOAD} is the electrical load power, kw.

- Thermal power balance constraint

$$H_{GT} + H_{EB} + H_{OUT} = H_{HLOAD} + H_{IN} \tag{12}$$

where H_{HLOAD} is the heat load power, kw.

- Natural gas power balance constraint

$$G_{GZ} + G_{OUT} + G_{P2G} = G_{GLOAD} + G_{IN} \tag{13}$$

where G_{GLOAD} is the gas load power, m^3.

- Equipment output constraint

$$P_{s,\min} \le P_{s,t} \le P_{s,\max} \tag{14}$$

where $P_{s,\min}$ and $P_{s,\max}$ denote the minimum and maximum values of the s-th equipment output, respectively, kw.

- Equipment climbing constraint.

$$-\Delta P_{s,\text{down}} \le P_{s,t+1} - P_{s,t} \le \Delta P_{s,\text{up}} \tag{15}$$

where $\Delta P_{s,\text{down}}$ and $\Delta P_{s,\text{up}}$ are the lower and upper limits of the sth equipment output creep, kw.

4. Results and Analysis

4.1. Typical Day Selection

Over the course of a year, the daily variation curves for electricity, heat, and gas loads, and for photovoltaic and wind turbine generation, are somewhat similar [24]. For the purposes of this study, a typical day for the load curve, *PV* generation curve, and WP generation curve is the day that is "closest" to the average fluctuation over the year.

For each day of the year, the daily curves for electricity, heat and gas loads, photovoltaics, and wind turbine generation in the area are first summarized separately.

$$C(n) = \frac{1}{N} \sum_{d=1}^{N} C(d, n) \tag{16}$$

From $C(d,n)$, the day curve $C(d^*,n)$ that is closest to the above $C(n)$ is then used as a typical day for load, PV, and WP generation, respectively. The definition of "closest" here means that the average deviation is minimal and is calculated as follows:

$$\sum_{n=1}^{24} |C(d^*,n) - C(n)| = \min_{1 \le d \le N} \sum_{n=1}^{24} |C(d,n) - C(n)| \tag{17}$$

The daily load, PV, and WT curves are subtracted from the respective average curves, and the date with the smallest sum of the absolute differences between the 24 moments of the day is taken as the respective typical day. Ultimately, a typical daily scenic output and load demand curve for the system is as shown in Figure 2.

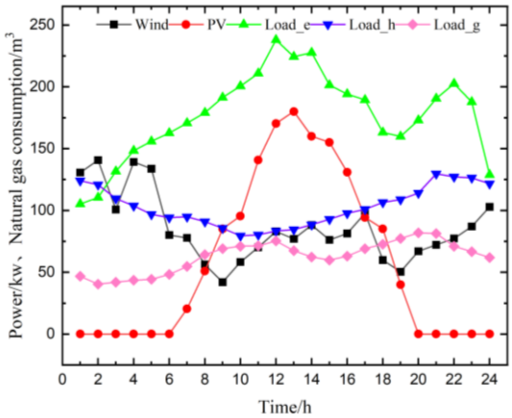

Figure 2. Typical daily scenario output and load capacity curve.

4.2. Simulation Parameters

In this paper, we combine the construction and operation data of an AIES containing HES and BG in a region with relevant literature data to set various parameters of the calculation case. The system parameters are shown in Table 1 [25–29]. The initial electricity storage state of the BES is 0.5, the initial heat storage state of the HST is 0.3, the initial gas storage state of the GST is 0.3, and the dispatching period is 1 h. The selling price of electricity at 00:00–06:00, 22:00–24:00 is 0.4 ¥/kw·h; that at 11:00–13:00, 18:00–20:00 is 1.35 ¥/kw·h; and the natural gas price is 3 ¥/m^3.

Table 1. System parameters.

Equipment	Capacity	Parameter	Value
MG-CHP/kw	110	η_E^{GT}	0.4
		η_{LOSS}^{GT}	0.05
		η_B	0.8
		C_{op}^{GT}	0.02
PV/kw	180	C_{op}^{PV}	0.15
WP/kw	160	C_{op}^{WIND}	0.03
BG/kw	30	$E_{BG,\max}$	600
		C_{op}^{BG}	0.02
EB/kw	40	η_{EB}	0.9
$P2G$/kw	120	η_{P2G}	0.5
		C_{op}^{P2G}	0.08

Table 1. *Cont.*

Equipment	Capacity	Parameter	Value
BES/kw·h	200	$\eta_C\eta_D$	0.95
		C_{op}^{ESS}	0.096
HST/kw·h	200	ϑ_{HS}	0.025
		$\eta_{IN}\eta_{OUT}$	0.98
GST/m^3	200	-	-

4.3. Analysis of Dispatching Results

(1) Electricity, heat, and gas load analysis

The outcomes of this AIES scheduling optimization are depicted in Figures 3–5. In terms of electrical power, WP, PV, and MG-CHP are the primary power supply devices. The BES and *P2G* devices assist in regulating system power. During the hours of 00:00–05:00 and 21:00–24:00, there is more wind power generation at night when the *EB* runs at full power. Thus, the output of MG-CHP and *BG* is smaller. The system purchases electricity at this time due to the lowest electricity price. Excess wind power is charged by BES and consumed by the *P2G* equipment. During the hours of 11:00–12:00 and 18:00–20:00, due to the highest electricity price and the largest electrical load, the power supply of MG-CHP and *BG* is increased and BES is discharged. The system creep is mainly borne by *BG* and BES. For the *P2G* equipment, it mainly works at the time when there is more renewable energy generation and electrical energy surplus to provide more renewable energy capacity and reduce the system operation cost. In terms of thermal, the *EB* and MG-CHP units bear the thermal baseload during the hours of 00:00–05:00 and 21:00–24:00, when the HST stores surplus thermal energy due to lower electricity. During the hours of 11:00–12:00 and 18:00–20:00, the MG-CHP units assume the thermal baseload and the HST assists in heating due to the highest electricity price and low thermal load. In terms of gas load, during the hours of 00:00–05:00 and 21:00–24:00, the system purchases large amounts of gas. The *P2G* unit uses excess clean electricity and low-priced electricity to produce gas, and the excess natural gas is stored in the storage tank. During the gas peak hours of midday and evening, the *P2G* unit and GST assist in supplying gas to reduce the system's gas purchase cost.

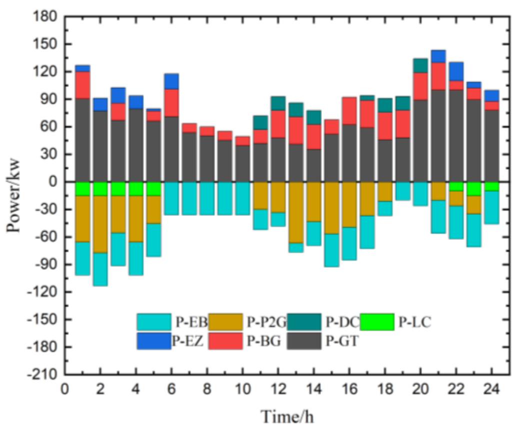

Figure 3. Power generation of each equipment and power purchase of the system.

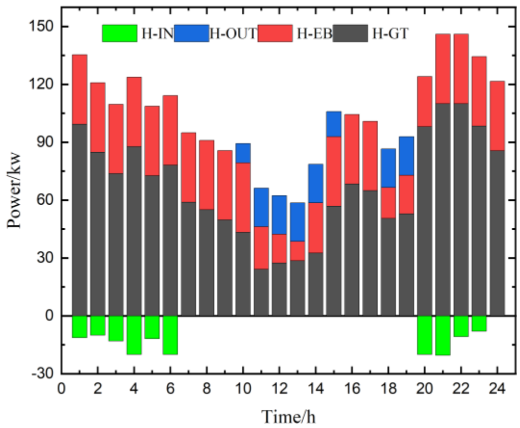

Figure 4. Heating capacity of each equipment.

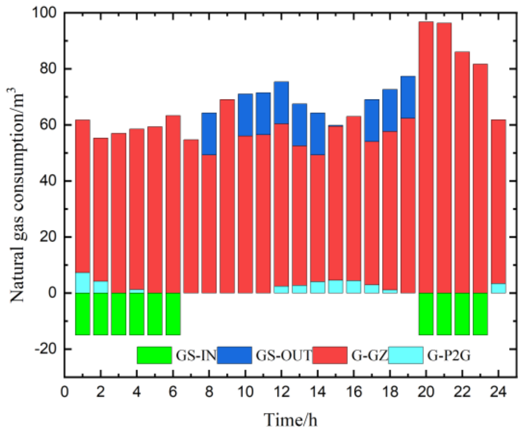

Figure 5. Gas production volume of equipment and gas purchase volume of the system.

(2) Comparative analysis of HES

As shown in Figure 6, the HST in the combined BES-HST energy storage has 10 h of non-operation and the total heat energy exchange and storage is reduced. Moreover, the charging and discharging power of BES fluctuates a great deal and it works for a long time. The power output of BES is dispersed during high electrical load hours. The reason for this phenomenon is that the addition of BES causes part of the electrical energy to be converted into thermal energy through *EB*, which causes the HST storage energy to decrease. The HST energy storage system is not active. As illustrated in Figure 7, with the combined BES-GST energy storage, the BES operates for an extended period of time, the capacity changes greatly, and electrical energy is converted into natural gas via *P2G* more frequently. Before the peak in gas load, BES discharges and GST stores natural gas to cope with the demand, but the fast charging and discharging of BES and GST will reduce the equipment life. Similarly, Figure 8 shows that in the HST-GST co-storage scenario, the actual release of HST equipment decreases and part of the demand is met by the GST equipment. Analyzing Figure 9, it can be seen that the charging period of BES-HST-GST joint storage occurs when the load is low and the electricity price is low. BES, HST, and GST follow the dynamic changes in the corresponding load. Compared with the rest of the combined energy storage, BES, HST, and GST can perform the system's peaking task better. Due to the addition of HST and GST, the conversion of electrical energy to heat and natural gas is reduced and the energy utilization efficiency is improved. Meanwhile, since the operating power of *P2G* and *EB* is positively correlated with the excess WP and *PV* generation, they can be regarded as an adjustable load on the grid side and an adjustable gas and heat source on the gas and heat network sides. The complementary operation of different energy systems not only makes it possible to reduce the cost of accommodating renewable energy generation, but also makes it possible to increase the system's backup capacity and flexibility significantly.

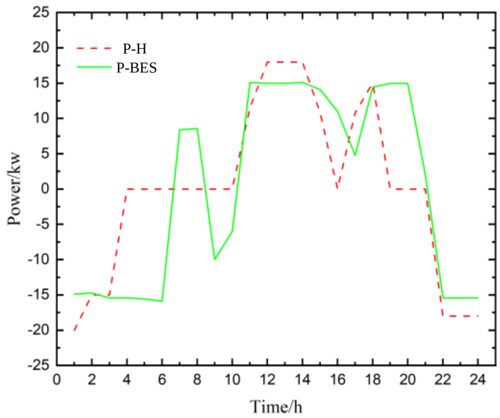

Figure 6. BES-HST joint output diagram.

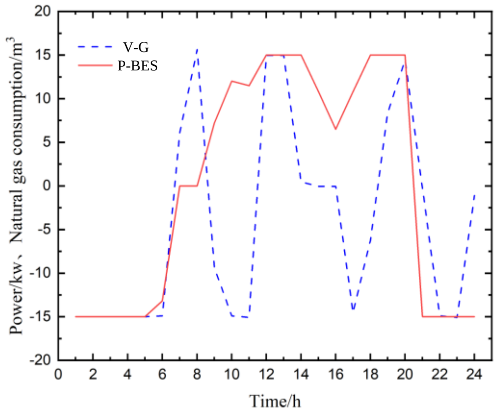

Figure 7. BES-GST joint output diagram.

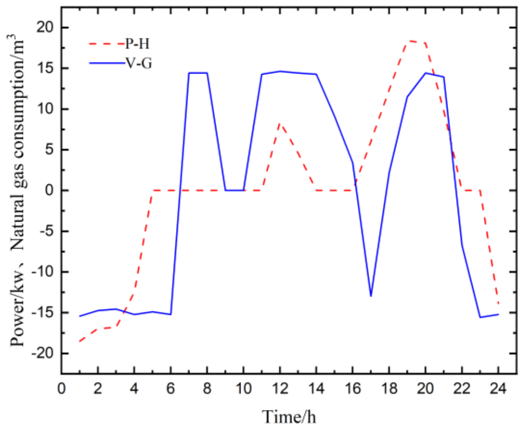

Figure 8. HST-GST joint output diagram.

(3) Operating cost analysis

An analysis of Table 2 shows that compared to an AIES with a single energy supply and no HES with the same parameters, the integrated cost of the optimized AIES is significantly reduced by around 20%. The environmental protection cost is reduced by around 23.2% because the system takes environmental protection into consideration. However, in order to ensure the energy demand of multiple loads, the AIES needs to purchase additional energy, and the cost of energy purchase increases by 4.1%. The energy efficiency coefficient is calculated with reference to the literature [30,31], and the optimized energy efficiency is improved by 51%, which shows that the AIES with HES can balance the economy and energy efficiency.

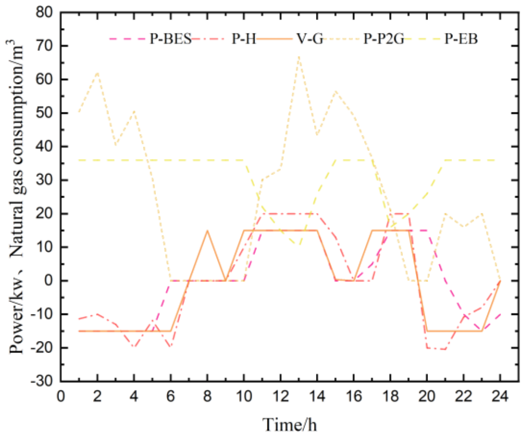

Figure 9. BES-HST-GST joint output diagram.

Table 2. Comparison of scenarios before and after optimization.

Comparison Items	AIES without HES	AIES with HES	Rate of Change
Comprehensive cost/¥	1.48×10^5	1.23×10^5	−20%
Energy purchase cost/¥	2.96×10^4	3.08×10^4	4.1%
Environmental protection costs/¥	2.43×10^4	1.87×10^4	23.2%
Energy efficiency factor/(kW·h)·kg^{-1}	6.791	10.236	51%

5. Conclusions

In this paper, considering the economic and environmental friendliness of AIES with HES, an optimal scheduling model of multi-energy complementarity is established with the maximum *PV* and WP accommodation as the premise, the minimum total cost of AIES operation as the objective function, and the *PV* and WP output prediction and load demand prediction curves as the input. By controlling the output of each piece of energy conversion equipment, the optimal system economy and environmental friendliness are improved. The main conclusions are as follows:

- Compared with the original system, the optimized system reduces the comprehensive cost by 20%, reduces the environmental protection cost by around 23.2%, and improves the energy efficiency by around 51%. The system can balance economy and energy utilization efficiency after introducing HES, *P2G*, and *EB* equipment.
- Under the HES mode, the output power of energy storage equipment is mainly based on the change in demand of the corresponding load, with fewer transformation times between different energies and less energy transformation loss.
- Multi-energy coupled AIES can realize low-cost renewable energy accommodation and can enhance the flexibility of system operation. At the same time, the efficiencies offered by AIES can lead to energy independence, economic competitiveness, job creation, and the more intelligent use of resources.

Author Contributions: Conceptualization, W.Y.; methodology, W.Y. and Y.X.; software, X.Y.; validation, H.Z., X.L. and H.M.; formal analysis, H.D.; investigation, Y.D.; resources, H.D.; data curation, W.Y.; writing—original draft preparation, W.Y.; writing—review and editing, Y.D; visualization, X.Y; supervision, H.M.; project administration, H.D. All authors have read and agreed to the published version of the manuscript.

Funding: This project is supported by the Technology Project of State Grid Gansu Electric Power Company (W22KJ2714016).

Data Availability Statement: Not applicable.

Conflicts of Interest: The authors declare no conflict of interest.

References

1. Ali, F.; Ahmar, M.; Jiang, Y.; AlAhmad, M. A techno-economic assessment of hybrid energy systems in rural Pakistan. *Energy* **2021**, *215*, 119103. [CrossRef]
2. Liu, Y.; Zang, Y.; Yang, Y. China's rural revitalization and development: Theory, technology and management. *J. Geogr. Sci.* **2020**, *30*, 1923–1942. [CrossRef]
3. MacDonald, S.; Winner, B.; Smith, L.; Juillerat, J.; Belknap, S. Bridging the rural efficiency gap: Expanding access to energy efficiency upgrades in remote and high energy cost communities. *Energy Effic.* **2020**, *13*, 503–521. [CrossRef]
4. Tan, C.; Yu, M.; Wang, J.; Geng, S.; Niu, D.; Tan, Z. Feasibility study on the construction of multi-energy complementary systems in rural areas—Eastern, central, and western parts of China are taken as examples. *Energy* **2022**, *249*, 123571. [CrossRef]
5. Sen, S.; Ganguly, S. Opportunities, barriers and issues with renewable energy development–A discussion. *Renew. Sustain. Energy Rev.* **2017**, *69*, 1170–1181. [CrossRef]
6. Li, J.; Wang, Z.; Cheng, X.; Shuai, J.; Shuai, C.; Liu, J. Has solar PV achieved the national poverty alleviation goals? Empirical evidence from the performances of 52 villages in rural China. *Energy* **2020**, *201*, 117631. [CrossRef]
7. Yanine, F.F.; Sauma, E.E. Review of grid-tie micro-generation systems without energy storage: Towards a new approach to sustainable hybrid energy systems linked to energy efficiency. *Renew. Sustain. Energy Rev.* **2013**, *26*, 60–95. [CrossRef]
8. Wang, Y.; Guo, L.; Ma, Y.; Han, X.; Xing, J.; Miao, W.; Wang, H. Study on operation optimization of decentralized integrated energy system in northern rural areas based on multi-objective. *Energy Rep.* **2022**, *8*, 3063–3084. [CrossRef]
9. Huang, Y.Q.; He, W.; Zhao, Z.W.; Li, J.; Rao, Z. Hierarchical Management for Rural Integrated Energy Systems Considering Dynamic Response Characteristics. *Proc. CSU-EPSA* **2022**, *34*. [CrossRef]
10. Mitali, J.; Dhinakaran, S.; Mohamad, A. Energy storage systems: A review. *Energy Storage Sav.* **2022**, *1*, 166–216. [CrossRef]
11. Kamal, M.M.; Ashraf, I.; Fernandez, E. Efficient two-layer rural electrification planning and techno-economic assessment integrating renewable sources. *Energy Storage* **2022**, *4*, e314. [CrossRef]
12. Kabeyi, M.J.B.; Olanrewaju, O.A. Biogas production and applications in the sustainable energy transition. *J. Energy* **2022**, *2022*, 8750221. [CrossRef]
13. Sodri, A.; Septriana, F.E. Biogas Power Generation from Palm Oil Mill Effluent (POME): Techno-Economic and Environmental Impact Evaluation. *Energies* **2022**, *15*, 7265. [CrossRef]
14. Ding, W.; Niu, H.; Chen, J.; Du, J.; Wu, Y. Influence of household biogas digester useon household energy consumption in a semi-arid rural region of northwest China. *Appl. Energy* **2012**, *97*, 16–23. [CrossRef]
15. Ahmed, J.; Harijan, K.; Shaikh, P.H.; Lashari, A.A. Techno-economic Feasibility Analysis of an Off-grid Hybrid Renewable Energy System for Rural Electrification. *J. Electr. Electron. Eng.* **2021**, *9*, 7. [CrossRef]
16. Bamisile, O.; Huang, Q.; Li, J.; Dagbasi, M.; Kemena, A.D.; Abid, M.; Hu, W. Modelling and performance analysis of an innovative CPVT, wind and biogas integrated comprehensive energy system: An energy and exergy approach. *Energy Convers. Manag.* **2020**, *209*, 112611. [CrossRef]
17. Teng, Y.; Wang, Z.; Li, Y.; Ma, Q.; Hui, Q.; Li, S. Multi-energy storage system model based on electricity heat and hydrogen coordinated optimization for power grid flexibility. *CSEE J. Power Energy Syst.* **2019**, *5*, 266–274. [CrossRef]
18. Yang, D.; Wang, M. Optimal operation of an integrated energy system by considering the multi energy coupling, AC-DC topology and demand responses. *Int. J. Electr. Power Energy Syst.* **2021**, *129*, 106826. [CrossRef]
19. Liu, J.; Sun, W.; Yan, J. Effect of P2G on Flexibility in Integrated Power-Natural Gas-Heating Energy Systems with Gas Storage. *Energies* **2021**, *14*, 196. [CrossRef]
20. Luo, F.; Shao, J.; Jiao, Z.; Zhang, T. Research on optimal allocation strategy of multiple energy storage in regional integrated energy system based on operation benefit increment. *Int. J. Electr. Power Energy Syst.* **2021**, *125*, 106376. [CrossRef]
21. Men, X.Y.; Cao, J.; Wang, Z.S.; Du, W.J. The constructing of multi-energy complementary system of energy internet microgrid and energy storage model analysis. *Proc. CSEE* **2018**, *38*, 5727–5737.
22. Zhe, Z. Multi-objective optimal dispatch of mining area integrated energy system with P2G and hybrid electric energy storage. *Electr. Power Autom. Equip.* **2021**, *41*, 8–15.
23. Rahman, A.; Farrok, O.; Haque, M. Environmental impact of renewable energy source based electrical power plants: Solar, wind, hydroelectric, biomass, geothermal, tidal, ocean, and osmotic. *Renew. Sustain. Energy Rev.* **2022**, *161*, 112279. [CrossRef]
24. Jiang, Z.; Li, S.; Ma, X.; Li, X.; Kang, Y.; Li, H.; Dong, H. State Estimation of Regional Power Systems with Source-Load Two-Terminal Uncertainties. *CMES-Comput. Modeling Eng. Sci.* **2022**, *132*, 295–317. [CrossRef]
25. Zhang, Z.; Zhang, Y.; Huang, Q.; Lee, W.-J. Market-oriented optimal dispatching strategy for a wind farm with a multiple stage hybrid energy storage system. *CSEE J. Power Energy Syst.* **2018**, *4*, 417–424. [CrossRef]
26. Li, G.; Zhang, R.; Jiang, T.; Chen, H.; Bai, L.; Cui, H.; Li, X. Optimal dispatch strategy for integrated energy systems with CCHP and wind power. *Appl. Energy* **2017**, *192*, 408–419. [CrossRef]
27. Alshammari, M.E.; Ramli MA, M.; Mehedi, I.M. Hybrid Chaotic Maps-Based Artificial Bee Colony for Solving Wind Energy-Integrated Power Dispatch Problem. *Energies* **2022**, *15*, 4578. [CrossRef]
28. Dong, Z.; Wong, K.P.; Meng, K.; Luo, F.; Yao, F.; Zhao, J. Wind power impact on system operations and planning. In Proceedings of the IEEE PES General Meeting, Minneapolis, MN, USA, 25–29 July 2010; pp. 1–5. [CrossRef]
29. Zakari, A.; Khan, I.; Tan, D.; Alvarado, R.; Dagar, V. Energy efficiency and sustainable development goals (SDGs). *Energy* **2022**, *239*, 122365. [CrossRef]

30. Hua, H.S.; Liu, Y.Q.; Xiong, W.; Xu, H.; Shi, Y.; Dong, S. Multi-objective optimized operation of energy system considering comprehensive energy efficiency. *South. Power Syst. Technol.* **2018**, *12*, 81–84.
31. Li, S.; Li, X.; Kang, Y.; Gao, Q. Load capability assessment and enhancement for transformers with integration of large-scale renewable energy: A brief review. *Front. Energy Res.* **2022**, *10*, 1002973. [CrossRef]